



Supported Co_3O_4 on expanded graphite as a catalyst for the degradation of Orange II in water using sulfate radicals

Penghui Shi^{a,b}, Shaobo Zhu^a, Hongai Zheng^{a,b}, Dengxin Li^{a,*}, Shihong Xu^a

^aCollege of Environment Science and Engineering, Donghua University, Shanghai 201620, P.R. China
Tel. +8621 6779 2514; email: lidengxin@dhu.edu.cn

^bCollege of Environmental and Chemical Engineering, Shanghai University of Electric Power, Shanghai 200090, P.R. China

Received 7 March 2013; Accepted 11 April 2013

ABSTRACT

A kind of heterogeneous catalysts is fabricated *in situ* by the decomposition of cobalt nitrate through heat and crystal growth of cobalt oxide (Co_3O_4) on the surface of expanded graphite (EG) in 1-hexanol solvent. The Co_3O_4 /EG catalyst can activate peroxydisulfate for the degradation of Orange II in water. The test results of X-ray diffraction, Fourier transform infrared spectroscopy, Raman spectroscopy (Raman), scanning electron microscopy, and high resolution transmission electron microscopy show that the Co_3O_4 /EG catalysts are EG decorated homogeneously with well-dispersed Co_3O_4 nanoparticles. The Co_3O_4 /EG catalysts exhibit an unexpectedly high catalytic activity than Co_3O_4 or EG alone in the degradation of Orange II in water by advanced oxidation processes based on sulfate radicals, and 100% decomposition can be achieved in 8 min. These phenomena suggest that there is a synergistic catalytic activity between Co_3O_4 and EG.

Keywords: Expanded graphite; Cobalt oxide; Sulfate radical; Advanced oxidation processes; Orange II

1. Introduction

Because of increasing public concerns and more strict regulations on harmful dye wastewater, it is important to develop efficient technologies for the complete removal of dye pollutants from wastewater. Over the past years, advanced oxidation processes (AOPs) based on the generation of sulfate radicals ($\text{SO}_4^{\cdot-}$) have emerged as a promising technique to degrade completely most dye pollutants [1–3]. Compared with $\cdot\text{OH}$ (1.7 eV), $\text{SO}_4^{\cdot-}$ has a higher oxidation potential (2.5–3.1 eV); hence, it has the potential to be

an efficient oxidant. The various combinations between the dissolved transition metal ions and oxidants have been evaluated systematically for the generation of active radicals by Dionysiou's group [1–3]. Peroxydisulfate (PMS) coupled with Co^{2+} ions is the best combination for the generation of $\text{SO}_4^{\cdot-}$ for degrading Orange II. However, due to the cobalt leachate, the oxidation using cobalt and PMS under a homogeneous system has profound disadvantage. The cobalt leachate is recognized as a priority metal pollutant. Therefore, the activation of PMS by

*Corresponding author.

heterogeneous cobalt sources has recently been paid great attention. Dionysiou et al. [4–6] studied both the unsupported and supported Co_3O_4 on several common supports (i.e. Al_2O_3 , SiO_2 , and TiO_2) as the heterogeneous activators for PMS to degrade 2,4-dichlorophenol. Kiwi et al. [7] used polytetrafluoroethylene flexible film as the support for Co_3O_4 nanoparticles to decompose organic dyes under light irradiation. Chen et al. [8] evaluated the performance of unsupported Co_3O_4 nanoparticles in the degradation of acid Orange 7. Zhang et al. [9] supported cobalt oxide on MgO for degradation of organic dyes in dilute solutions, and Shukla et al. [10] studied cobalt exchanged zeolites for heterogeneous catalytic oxidation of phenol in the presence of peroxy monosulphate. So, seeking a perfect catalyst support is the important challenge for the specialists and scholars, and a perfect catalyst support can solve the problem of dissolving out cobalt.

Carbon materials have long been used as catalyst support in heterogeneous catalysis as they satisfy most of the characteristics required for chemical inertness (resistance to both acidic and basic media), porosity, large surface area, and facility in recovery of metals, especially precious metals by support burning [11]. There are several types of carbon materials, such as activated carbon, activated carbon fiber, graphite, carbon black, graphite intercalation compounds, carbon nanotubes, magnetically separable carbon materials, graphene, graphene oxide, reduced graphene oxide, etc. have been used as catalyst support [12–28]. Although they perform well as catalyst support, their high cost and complex production process have limited their practical utility in industrial catalysis, especially graphene, graphene oxide, or reduced graphene oxide, even though they have hidden potential. So, a low-cost and stable performance catalyst support is urgently needed. Expanded graphite (EG) is an important carbon material which has the properties of high temperature resistance, oxidation resistance, corrosion resistance, radiation resistance, and good thermal conductivity. Meanwhile, the EG has a unique network-like pore structure with larger surface area and higher surface activity, which is perfectly suitable for using as catalyst support [29–31]. In this paper, we supported Co_3O_4 on EG as a highly efficient catalysts for the removal of Orange II from water.

Orange II (Fig. 1) as a synthetic azo dye is widely used. It cannot be degraded through biological methods, resists light irradiation, and chemical oxidation. It is usually used as a model substrate for the aromatic azo dyes. Therefore, more and more scholars began studying the degradation of Orange II. Kiwi et al. [32]

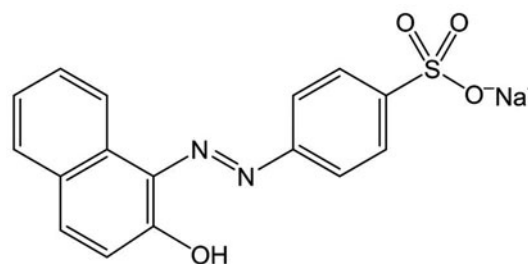


Fig. 1. Molecular structure of Orange II.

reported a catalytic photoassisted system, Fe^{3+} /nafion/glass fibers. Ramirez et al. [33–38] investigated optimum conditions for Fenton's oxidation and applied a heterogeneous catalytic wet hydrogen peroxide process based on saponite clay. Kousha et al. [39] used raw and chemically modified brown macroalga, *Stoehospermum marginatum*, to adsorb acid Orange II dye. Mandal et al. [40] revealed that the alginate–clay composites had high adsorption capacity for the adsorption of Orange II dye from aqueous solutions. Riaz et al. [41] used bimetallic Cu–Ni/ TiO_2 under visible light. Liang et al. [42] applied chromium substituted magnetite as heterogeneous Fenton catalyst for the degradation of Orange II.

Therefore, in the present paper, we will report an efficient heterogeneous catalyst, that supported Co_3O_4 on EG, for activation of PMS and use in the degradation of Orange II in water by AOPs based on sulfate radicals and discuss its performance as a novel catalyst support.

2. Experimental

2.1. Materials

Expansible graphite was supplied by Shanghai Yifan Graphite Co. Ltd., China. Orange II (98% purity) was supplied by Shanghai Yiji Dye Chemicals. PMS, available as a triple salt of sulfate commercially known as oxone ($2\text{KHSO}_5 \cdot \text{KHSO}_4 \cdot \text{K}_2\text{SO}_4$, 4.5–4.9% active oxygen), was obtained from Shanghai Ansin Chemical Co. Ltd. and used as an oxidant. Other reagents including 1-hexanol solvent, $\text{Co}(\text{NO}_3)_2 \cdot 6\text{H}_2\text{O}$, H_2SO_4 (98%), NaNO_3 , KMnO_4 , and H_2O_2 (30%) of analytical grade were provided by Sinopharm Chemical Reagent Co. Ltd. (China).

2.2. Preparation of $\text{Co}_3\text{O}_4/\text{EG}$

EG was prepared by heating the expansible graphite to $1,200^\circ\text{C}$ for 10 s. In the preparation of $\text{Co}_3\text{O}_4/$

EG, EG (100 mg) was dispersed into 30 mL of 1-hexanol solvent through sonication for 3 h. Meanwhile, 0.5 mmol $\text{Co}(\text{NO}_3)_2 \cdot 6\text{H}_2\text{O}$ was dissolved into another 20 mL of 1-hexanol solvent. The mixture was magnetically stirred for 2 h, and the resulting mixture was heated to 140°C under vigorous magnetic stirring for 12 h. After the system was cooled to room temperature, the suspension was centrifuged, washed with absolute ethanol and water several times until all the remaining 1-hexanol solvent alcohol and other sundries were removed, and dried in a vacuum oven at 60°C for 24 h. The product was labeled as $\text{Co}_3\text{O}_4/\text{EG}$. In addition, Co_3O_4 was synthesized with the same parameters for comparison [43].

2.3. Characterization and technique

The structural features and the mineralogy were studied using X-ray diffraction (XRD) patterns obtained on a RIGAKU XRD instrument, using filtered $\text{CuK}\alpha$ radiation with accelerating voltage of 40 kV and current of 200 mA. The sample was scanned at 2θ from 5° to 90°.

The changes in the surface chemical bondings and surface composition were characterized by Fourier transform infrared spectroscopy (FTIR; Bruker, Tensor 27), which were obtained to prove the success of supporting cobalt oxide on EG. The test samples were pressed into tablets with KBr.

Raman spectroscopy was performed on a Nicolet Micro-Raman (NEXUS-670, USA).

The texture, morphology, and semi-quantitative analyses were performed using scanning electron microscopy (SEM, JEOL JSM-5600LV) with both secondary and backscatter electrons.

The nanoscale structures were observed using high resolution transmission electron microscopy (FE-HRTEM, JEOL JEM-2100F) with an accelerating voltage of 200 kV. The sample was prepared by dispersing a small amount of dry powder in ethanol or water. Then, one droplet of the suspension was dropped on a formvar-carbon-coated, 300 mesh copper TEM grids (Ted Pella) covered with thin amorphous carbon film and allowed to evaporate in air at room temperature.

2.4. Evaluation of catalytic activity

The degradation experiments were conducted in a 250 mL vessel. In a typical reaction of Orange II degradation with 0.2 mM, 0.1 g/L of catalyst and 1 mM of oxone were added. Samples were obtained at regular intervals, joined immediately with NaNO_2 (5 g/L) as quencher, and then filtered using a 0.22 μm filtering membrane. Orange II concentration in the filtrate was

measured in a UV-Vis spectrophotometer (Xinmao 7504) at 486 nm. Commercial oxone can be used to generate PMS, and 614.7 g/L (1 M) of oxone is necessary to release 2 M PMS. The vessel was placed in a water-bathing constant-temperature vibrator controlled at 25°C throughout the process. For the purpose of practical application, the additional sulfate ions released by oxone can be reclaimed by ion exchange resin. The experiment was conducted under neutral (pH 7.0, adjusted with bicarbonate solution) conditions. And most of the experiments were conducted in triplicate. For a comparison, the experiment on the catalytic activity of EG and Co_3O_4 in the presence of PMS was conducted in the same conditions.

The catalyst was collected by centrifugation and thoroughly washed with distilled water and ethanol after each run during the recycling experiment of the catalyst. Then, the catalyst was dried in a vacuum oven at 60°C for 24 h to remove excess water and ethanol. Because certain catalyst loss was unavoidable during the washing and drying process, several parallel reactions were conducted in the first three runs to ensure that the recycled catalyst amount was enough for the next run. Catalyst dose and other reaction conditions were maintained for the subsequent runs.

3. Results and discussion

3.1. Characterizations of composites

The structural properties of the $\text{Co}_3\text{O}_4/\text{EG}$ were analyzed and compared with those of EG by XRD (Fig. 2). EG showed a very sharp diffraction peak at $2\theta = 26.26^\circ$ and showed a weak diffraction peak at $2\theta = 54.72^\circ$, which was the same as graphite. It indicated that the structural features and the mineralogy

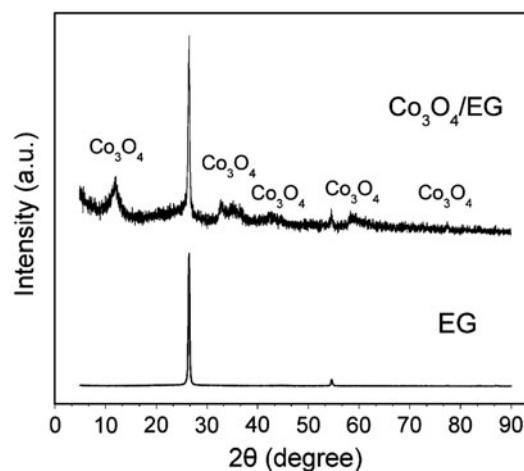


Fig. 2. XRD patterns of EG and $\text{Co}_3\text{O}_4/\text{EG}$.

of EG are similar to those of natural graphite. By contrast, the spectra of the $\text{Co}_3\text{O}_4/\text{EG}$ showed distinct peaks of EG at 26.26° and 54.72° , and cobalt oxide crystallites (Co_3O_4) at 12.7° , 32.8° , 36.8° , 44.8° , 58.4° , and 75.6° . The relative weak intensity of the peaks demonstrates that the Co_3O_4 particles have small sizes. The XRD analysis results indicate that the chemical composition and structural properties of $\text{Co}_3\text{O}_4/\text{EG}$ should be very different from that of the pure EG. And no peaks from other phases have been detected, indicating that the product is of high purity.

The FTIR spectra of EG, Co_3O_4 , and $\text{Co}_3\text{O}_4/\text{EG}$ are presented in Fig. 3. The band at $3,439$ and $1,385\text{ cm}^{-1}$ in the IR spectrum of EG are attributed to O–H stretching and bending vibration, respectively. The band at $1,630\text{ cm}^{-1}$ corresponds to the skeletal vibrations of graphitic domains. The IR spectrum of Co_3O_4 shows strong absorptions at 663 and 581 cm^{-1} due to Co_3O_4 . By contrast, the FTIR spectra of $\text{Co}_3\text{O}_4/\text{EG}$ differed from that of EG as shown by the weakening of the peaks of O–H stretching and bending vibration at $1,632$ and $3,435\text{ cm}^{-1}$, respectively. They also showed strong absorptions at 662 and 573 cm^{-1} because of the formation of Co_3O_4 , confirming the existence of Co_3O_4 . In addition, a new absorption band at approximately $1,049\text{ cm}^{-1}$ in the IR spectrum of the residual sediment may be attributed to C–O.

Raman spectroscopy is a powerful nondestructive tool used to distinguish ordered and disordered crystal structures of carbonaceous materials. The G band is common to all sp^2 carbon forms and provides information on the in-plane E_{2g} phonon of sp^2 bonded carbon atoms, whereas the D band is a breathing mode of the k -point phonons of A_{1g} symmetry [44–48]. Fig. 4 shows the Raman spectra of $\text{Co}_3\text{O}_4/\text{EG}$, which exhib-

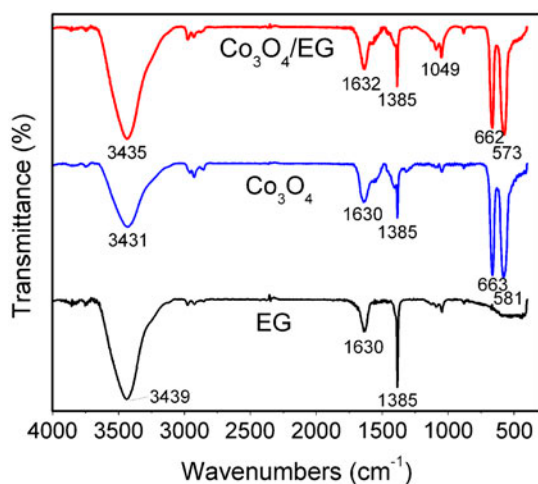


Fig. 3. FTIR spectra of EG, Co_3O_4 , and $\text{Co}_3\text{O}_4/\text{EG}$.

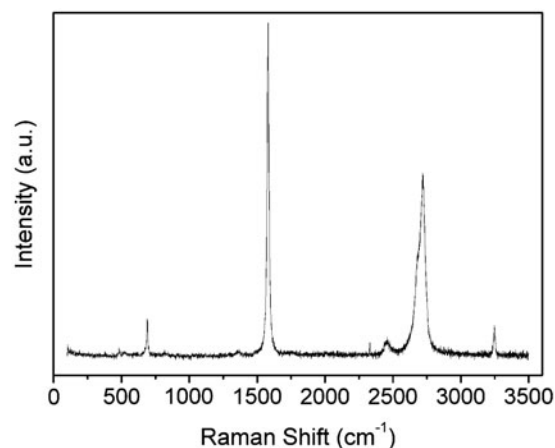


Fig. 4. Raman spectra of $\text{Co}_3\text{O}_4/\text{EG}$.

ited a strong G band at $1,580\text{ cm}^{-1}$. The 2D band at $2,719\text{ cm}^{-1}$ is the most prominent feature in the Raman spectrum of $\text{Co}_3\text{O}_4/\text{EG}$. And the obvious Raman peaks at 689.7 cm^{-1} assigned to the Raman active modes of Co_3O_4 were also observed.

The typical SEM images (Fig. 5) show the morphology of the synthesized EG and $\text{Co}_3\text{O}_4/\text{EG}$. The pore structure in EG is distributed uniformly with thin walls and loose structures containing multipores. (Fig. 5(a)). As shown in Fig. 5(a), EG had a honeycomb substructure with many diamond-shaped pores. The extensively expanded layers in nanometer thicknesses and highly open spaces between layers, which were suitable to load and disperse Co_3O_4 on EG during impregnation, facilitated the processing and formation of *in situ* $\text{Co}_3\text{O}_4/\text{EG}$ composites. In contrast to the surface of EG which was quite smooth (Fig. 5(a)), the Co_3O_4 added on EG appeared as bright dots uniformly spread over the surface of EG (Fig. 5(b)). But there was also agglomeration of the Co_3O_4 nanoparticles on EG.

The TEM images (Fig. 6) can provide better qualitative understanding of the internal structure and spatial distribution, as well as dispersion of Co_3O_4 anchored on the surface of EG, through direct visualization. The brighter grayish domains corresponded to EG support, whereas the darker dots were Co_3O_4 nanoparticles (Fig. 6(a)). It could be observed that the Co_3O_4 particles were well dispersed on EG surface with the size of about 3–5 nm and the lattice fringes of Co_3O_4 are about 0.184 nm. Meanwhile, the thermogravimetric analysis of $\text{Co}_3\text{O}_4/\text{EG}$ indicated a quality score of about 38 wt.% for Co_3O_4 in the $\text{Co}_3\text{O}_4/\text{EG}$ material.

3.2. Degradation of Orange II performances

The degradation or adsorption curves of Orange II under different conditions are shown in Fig. 7. All of

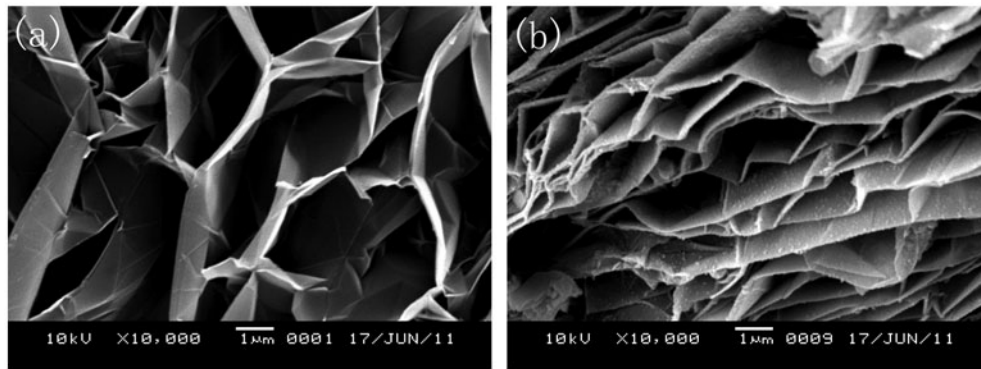


Fig. 5. SEM images of the synthesized EG (a) and Co₃O₄/EG (b).

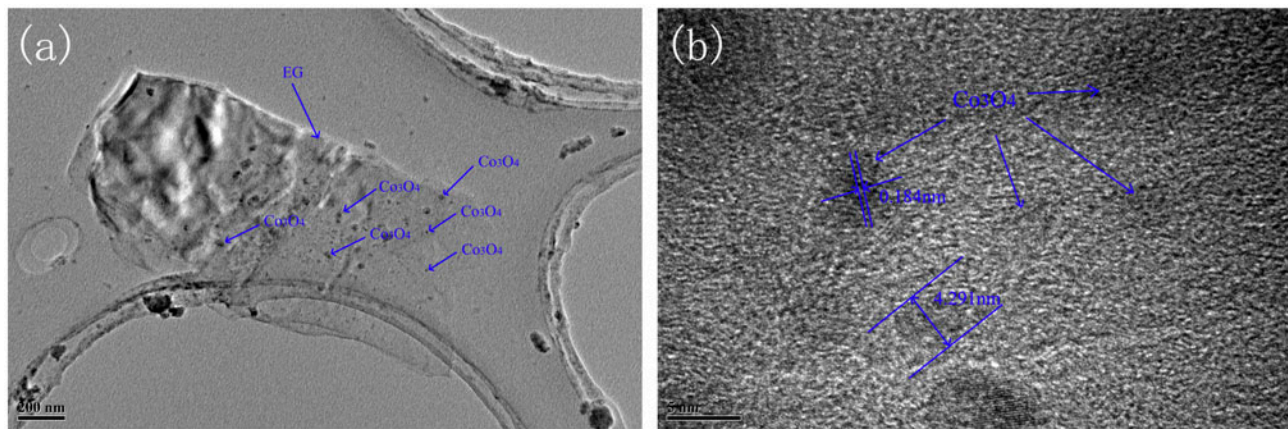


Fig. 6. TEM images of Co₃O₄/EG with low (a) and high magnification (b).

the experiments were conducted in neutral conditions with the catalyst dosage of 0.1 g/L and the pH during the entire reaction process was almost constant. Curves a, b, and c indicated the adsorption of Orange II onto Co₃O₄, EG, and Co₃O₄/EG, respectively. Each of them had a little adsorption and reached a balance after some time. The adsorptive capacity of Co₃O₄/EG was stronger than EG and EG was stronger than Co₃O₄. The concentration of Orange II only decreased around 45% in the first few minutes and then a plateau was reached after about 24 min for Co₃O₄/EG. So, an obvious extent of adsorption occurred without PMS which could be due to the physical adsorption on the surface of Co₃O₄/EG, EG, or Co₃O₄. In the reaction liquid (with 2 mM PMS and without a catalyst), the degradation occurred very slowly and approximately 47% of Orange II was degraded in the first 60 min (curve d). Curves e and f indicate the catalytic activity of EG and unsupported Co₃O₄, respectively. Both EG and Co₃O₄ displayed a certain catalytic activity in the presence of PMS. However, there is still 40% of Orange II remaining in the first

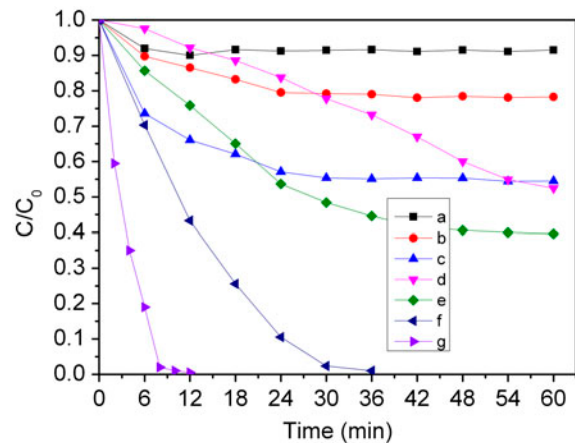


Fig. 7. Degradation curves of Orange II under different conditions: (a) [Co₃O₄]=0.1 g/L; (b) [EG]=0.1 g/L; (c) [Co₃O₄/EG]=0.1 g/L; (d) [PMS]=2 mM; (e) [EG]=0.1 g/L and [PMS]=2 mM; (f) [Co₃O₄]=0.1 g/L and [PMS]=2 mM, and (g) [Co₃O₄/EG]=0.1 g/L and [PMS]=2 mM.

60 min using EG as catalyst and the Orange II degradation rate can reach 100% within 36 min using Co_3O_4 as catalyst. Therefore, it confirms that the quick decrease of Orange II concentration is due to the degradation of Orange II rather than adsorption. Curve g shows that Orange II can be thoroughly degraded within about 8 min using $\text{Co}_3\text{O}_4/\text{EG}$ as catalyst. Thus, the $\text{Co}_3\text{O}_4/\text{EG}$ catalyst prepared in this work has the very good catalytic effect. The $\text{Co}_3\text{O}_4/\text{EG}$ catalysts exhibit an unexpectedly high catalytic activity than Co_3O_4 or EG alone suggesting synergistic coupling between Co_3O_4 and EG is indispensable to the high catalytic activity of the hybrid.

3.3. Stability of $\text{Co}_3\text{O}_4/\text{EG}$ in multiple runs

Four recycling runs of the $\text{Co}_3\text{O}_4/\text{EG}$ were performed and the catalyst under the same reaction conditions to evaluate the stability of the $\text{Co}_3\text{O}_4/\text{EG}$ catalyst. The activity of the catalyst dropped compared with the fresh catalyst in the before cycling (Fig. 8). The leaching of cobalt ions from the used catalyst increased slightly when compared to the previous runs detected through inductively coupled plasma. And the surface area measurement of the fresh and used catalyst after the first run via nitrogen gas absorption yielded a Brunauer, Emmett & Teller, specific surface area value of 58.3 and 21.2 m^2/g , and the surface area decreased obviously. Therefore, both the leaching of cobalt and the reduction of the surface area might be responsible for the activity decay. However, although the activity of the catalyst drops, 100% degradation of Orange II can also be reached within 60 min after four cycling.

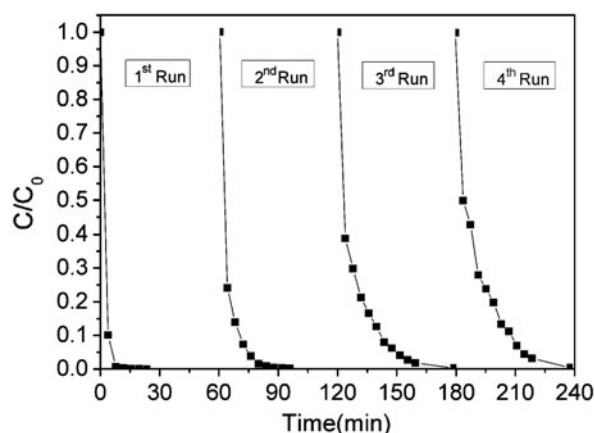


Fig. 8. Degradation of Orange II in consecutive runs using the recycled $\text{Co}_3\text{O}_4/\text{EG}$ catalyst at neutral pH, $[\text{Orange II}]_0 = 0.2 \text{ mM}$, $[\text{Co}_3\text{O}_4/\text{EG}] = 0.1 \text{ g/L}$, and $[\text{PMS}] = 2 \text{ mM}$.

4. Conclusions

The $\text{Co}_3\text{O}_4/\text{EG}$, prepared in a solvothermal system, is a highly efficient catalyst and can accomplish the degradation of Orange II within 8 min used in AOPs based on $\text{SO}_4^{\cdot-}$ as a heterogeneous catalyst. It also exhibits a markedly better efficiency for PMS activation than unsupported Co_3O_4 catalyst. XRD, FTIR, Raman, SEM, and TEM indicated that the structure of the $\text{Co}_3\text{O}_4/\text{EG}$ is stable, and the well-dispersed nanoscale Co_3O_4 particles (3–5 nm) on EG indicates a high surface area, excellent structure, and perfect catalytic properties. Meanwhile, $\text{Co}_3\text{O}_4/\text{EG}$ exhibited an unexpected high catalytic activity than unsupported Co_3O_4 and EG alone. Thus, Co_3O_4 supported on EG is a synergistic catalyst for degradation of Orange II in water by AOPs based on sulfate radicals.

Acknowledgements

The study was supported by the Fundamental Research Funds for the Central Universities (12D11319), Shanghai Tongji Gao Tingyao Environmental Science & Technology Development Foundation (STGEF), Innovation Program of Shanghai Municipal Education Commission (12ZZ069), Shanghai Municipal Natural Science Foundation (No. 11ZR1400400), Fundamental Research Funds for the Central Universities (No. 11D11303), and Shanghai Leading Academic Discipline Project (No. B604).

References

- [1] G.P. Anipsitakis, D.D. Dionysiou, Degradation of organic contaminants in water with sulfate radicals generated by the conjunction of peroxymonosulfate with cobalt, *Environ. Sci. Technol.* 37 (2003) 4790–4797.
- [2] G.P. Anipsitakis, D.D. Dionysiou, Transition metal/UV-based advanced oxidation technologies for water decontamination, *Appl. Catal. B* 54 (2004) 155–163.
- [3] G.P. Anipsitakis, D.D. Dionysiou, Radical generation by the interaction of transition metals with common oxidants, *Environ. Sci. Technol.* 38 (2004) 3705–3712.
- [4] Q.J. Yang, H. Choi, Y.J. Chen, D.D. Dionysiou, Heterogeneous activation of peroxymonosulfate by supported cobalt catalysts for the degradation of 2,4-dichlorophenol in water: The effect of support, cobalt precursor, and UV radiation, *Appl. Catal. B* 77 (2008) 300–307.
- [5] Q.J. Yang, H. Choi, D.D. Dionysiou, Nanocrystalline cobalt oxide immobilized on titanium dioxide nanoparticles for the heterogeneous activation of peroxymonosulfate, *Appl. Catal. B* 74 (2007) 170–178.
- [6] G.P. Anipsitakis, E. Stathatos, D.D. Dionysiou, Heterogeneous activation of oxone using Co_3O_4 , *J. Phys. Chem. B* 109 (2005) 13052–13055.
- [7] P. Raja, M. Bensimon, U. Klehm, P. Albers, D. Laub, L. Kiwi-Minsker, A. Renken, J. Kiwi, Highly dispersed PTFE/ Co_3O_4 flexible films as photocatalyst showing fast kinetic performance for the discoloration of azo-dyes under solar irradiation, *J. Photochem. Photobiol. A* 187 (2007) 332–338.
- [8] X.Y. Chen, J.W. Chen, X.L. Qiao, D.G. Wang, X.Y. Cai, Performance of nano- Co_3O_4 /peroxymonosulfate system: Kinetics and mechanism study using acid Orange 7 as a model compound, *Appl. Catal. B* 80 (2008) 116–121.

- [9] W. Zhang, H.L. Tay, S.S. Lim, Y.S. Wang, Z.Y. Zhong, R. Xu, Supported cobalt oxide on MgO: Highly efficient catalysts for degradation of organic dyes in dilute solutions, *Appl. Catal. B* 95 (2010) 93–99.
- [10] P. Shukla, S.B. Wang, K. Singh, H.M. Ang, M.O. Tadé, Cobalt exchanged zeolites for heterogeneous catalytic oxidation of phenol in the presence of peroxymonosulphate, *Appl. Catal. B* 99 (2010) 163–169.
- [11] W. Li, C. Han, W. Liu, M.H. Zhang, K.Y. Tao, Expanded graphite applied in the catalytic process as a catalyst support, *Catal. Today* 125 (2007) 278–281.
- [12] R.R. Francisco, The role of carbon materials in heterogeneous catalysis, *Carbon* 36 (1998) 159–175.
- [13] Z.G. Zhang, N. Zhang, J. Peng, X.M. Fang, X.N. Gao, Y.T. Fang, Preparation and thermal energy storage properties of paraffin/expanded graphite composite phase change material, *Appl. Energy* 91 (2012) 426–431.
- [14] P. Serp, M. Corrias, P. Kalck, Carbon nanotubes and nanofibers in catalysis, *Appl. Catal. A* 253 (2003) 337–358.
- [15] J.M. Nhut, L. Pesant, J.P. Tessonnier, G. Winé, J. Guille, P.H. Cuong, M.J. Ledoux, Mesoporous carbon nanotubes for use as support in catalysis and as nanosized reactors for one-dimensional inorganic material synthesis, *Appl. Catal. A* 254 (2003) 345–363.
- [16] Y. Kong, X.H. Chen, J.H. Ni, S.P. Yao, W.C. Wang, Z.Y. Luo, Z.D. Chen, Palygorskite–expanded graphite electrodes for catalytic electro-oxidation of phenol, *Appl. Clay Sci.* 49 (2010) 64–68.
- [17] J.G. Zhao, Y. Guo, F. Feng, Q.H. Tong, W.S. Qv, H.Q. Wang, Microstructure and thermal properties of a paraffin/expanded graphite phase-change composite for thermal storage, *Renewable Energy* 36 (2011) 1339–1342.
- [18] Y.L. Min, K. Zhang, W. Zhao, F.C. Zheng, Y.C. Chen, T.G. Zhang, Enhanced chemical interaction between TiO₂ and graphene oxide for photocatalytic decolorization of methylene blue, *Chem. Eng. J.* 193–194 (2012) 203–210.
- [19] C.J. Madarang, H.Y. Kim, G.H. Gao, N. Wang, J. Zhu, H. Feng, M. Goring, M.L. Kasner, S.F. Hou, Adsorption behavior of EDTA-graphene oxide for Pb (II) removal, *Appl. Mater. Interfaces* 4 (2012) 1186–1193.
- [20] A.R. Marlinda, N.M. Huang, M.R. Muhamad, M.N. Anamt, B.Y.S. Chang, N. Yusoff, I. Harrison, H.N. Lim, C.H. Chia, S. V. Kumar, Highly efficient preparation of ZnO nanorods decorated reduced graphene oxide nanocomposites, *Mater. Lett.* 80 (2012) 9–12.
- [21] B. Kulic, S. Sencanli, Ö. Metin, Hydrolytic dehydrogenation of ammonia borane catalyzed by reduced graphene oxide supported monodisperse palladium nanoparticles: High activity and detailed reaction kinetics, *J. Mol. Catal. A: Chem.* 361–362 (2012) 104–110.
- [22] L.L. Fan, C.N. Luo, M. Sun, X.J. Li, F.G. Lu, H.M. Qiu, Preparation of novel magnetic chitosan/graphene oxide composite as effective adsorbents toward methylene blue, *Bioresour. Technol.* 114 (2012) 703–706.
- [23] J.F. Wang, T. Tsuzuki, B. Tang, X.L. Hou, L. Sun, X.G. Wang, Reduced graphene oxide/ZnO composite: Reusable adsorbent for pollutant management, *ACS Appl. Mater. Interfaces* 4 (2012) 3084–3090.
- [24] Y.Q. Sun, Q. Wu, G.Q. Shi, Graphene based new energy materials, *Energy Environ. Sci.* 4 (2011) 1113–1132.
- [25] P. Shukla, S.B. Wang, H.Q. Sun, H.M. Ang, M.O. Tadé, Activated carbon supported cobalt catalysts for advanced oxidation of organic contaminants in aqueous solution, *Appl. Catal. B* 100 (2010) 529–534.
- [26] Y. Hardjono, H.Q. Sun, H.Y. Tian, C.E. Buckley, S.B. Wang, Synthesis of Co oxide doped carbon aerogel catalyst and catalytic performance in heterogeneous oxidation of phenol in water, *Chem. Eng. J.* 174 (2011) 376–382.
- [27] H.Q. Sun, S.Z. Liu, G.L. Zhou, H.M. Ang, M.O. Tadé, S.B. Wang, Metal-free graphene catalyzed activation of peroxy-monosulfate (PMS) for green remediation of water, *ACS Appl. Mater. Interface* 4 (2012) 5466–5471.
- [28] Y.J. Yao, Z.H. Yang, H.Q. Sun, S.B. Wang, Hydrothermal synthesis of Co₃O₄–graphene for heterogeneous activation of peroxy-monosulfate for decomposition of phenol, *Ind. Eng. Chem. Res.* 51 (2012) 14958–14965.
- [29] Y. Kong, Y.Y. Xu, H.H. Mao, C. Yao, X.F. Ding, Expanded graphite modified with intercalated montmorillonite for the electrochemical determination of catechol, *J. Electroanal. Chem.* 669 (2012) 1–5.
- [30] G.L. Wang, Q.R. Sun, Y.Q. Zhang, J.H. Fan, L.M. Ma, Sorption and regeneration of magnetic exfoliated graphite as a new sorbent for oil pollution, *Desalination* 263 (2010) 183–188.
- [31] A.S. Tikhomirov, N.E. Sorokina, O.N. Shornikova, V.A. Morozov, G. Van Tendeloo, V.V. Avdeev, The chemical vapor infiltration of exfoliated graphite to produce carbon/carbon composites, *Carbon* 49 (2011) 147–153.
- [32] J. Kiwi, M.R. Dhananjeyan, J. Albers, O. Enea, Photo-assisted immobilized Fenton degradation up to pH8 of azo dye Orange II mediated by Fe³⁺/nafion/glass fibers, *Helv. Chim. Acta* 84 (2001) 3433–3445.
- [33] J.H. Ramirez, F.J. Maldonado-Hodar, A.F. Perez-Cadenas, Azo-dye Orange II degradation by heterogeneous Fenton-like reaction using carbon–Fe catalysts, *Appl. Catal. B* 75 (2007) 312–323.
- [34] J.H. Ramirez, C.A. Costa, L.M. Madeira, Experimental design to optimize the degradation of the synthetic dye Orange II using Fenton's reagent, *Catal. Today* 107–108 (2005) 68–76.
- [35] J.H. Ramirez, C.A. Costa, L.M. Madeira, G. Mata, M.A. Vicente, M.L. Rojas-Cervantes, A.J. Lopez-Peinado, R.M. Martin-Aranda, Fenton-like oxidation of Orange II solutions using heterogeneous catalysts based on saponite clay, *Appl. Catal. B* 71 (2007) 44–56.
- [36] J.H. Ramirez, F.M. Duarte, F.G. Martins, C.A. Costa, L.M. Madeira, Modelling of the synthetic dye Orange II degradation using Fenton's reagent: From batch to continuous reactor operation, *Chem. Eng. J.* 148 (2009) 394–404.
- [37] A.M.T. Silva, J.H. Ramirez, U. Söylemez, L.M. Madeira, A lumped kinetic model based on the Fermi's equation applied to the catalytic wet hydrogen peroxide oxidation of acid Orange 7, *Appl. Catal. B* 121–122 (2012) 10–19.
- [38] J.H. Ramirez, A.M.T. Silva, M.A. Vicente, C.A. Costa, L.M. Madeira, Degradation of acid Orange 7 using a saponite-based catalyst in wet hydrogen peroxide oxidation: Kinetic study with the Fermi's equation, *Appl. Catal. B* 101 (2011) 197–205.
- [39] M. Kousha, E. Daneshvar, M.S. Sohrabi, M. Jokar, A. Bhatnagar, Adsorption of acid Orange II dye by raw and chemically modified brown macroalga *Stoechospermum marginatum*, *Chem. Eng. J.* 192 (2012) 67–76.
- [40] S. Mandal, V.S. Patil, S. Mayadevi, Alginate and hydrotalcite-like anionic clay composite systems: Synthesis, characterization and application studies, *Microporous Mesoporous Mater.* 158 (2012) 241–246.
- [41] N. Riaz, N. Chong, B.K. Dutta, Z.B. Man, M.S. Khan, E. Nur-laela, Photodegradation of Orange II under visible light using Cu–Ni/TiO₂: Effect of calcination temperature, *Chem. Eng. J.* 185–186 (2012) 108–119.
- [42] X.L. Liang, Y.H. Zhong, H.P. He, P. Yuan, J.X. Zhu, S.Y. Zhu, Z. Jiang, The application of chromium substituted magnetite as heterogeneous Fenton catalyst for the degradation of aqueous cationic and anionic dyes, *Chem. Eng. J.* 191 (2012) 177–184.
- [43] T. He, D.R. Chen, X.L. Jiao, Controlled synthesis of Co₃O₄ nanoparticles through oriented aggregation, *Chem. Mater.* 16 (2004) 737–743.

- [44] F. Tuinstra, J.L. Koenig, Raman spectrum of graphite, *J. Chem. Phys.* 53 (1970) 1126–1130.
- [45] C. Wang, L. Zhan, W.M. Qiao, L.C. Ling, Preparation of graphene nanosheets through detonation, *New Carbon Mater.* 26 (2011) 21–25.
- [46] M.S. Dresselhaus, A. Jorio, M. Hofmann, G. Dresselhaus, R. Saito, Perspectives on carbon nanotubes and graphene Raman spectroscopy, *Nano Lett.* 10 (2010) 751–758.
- [47] W.X. Zhang, J.C. Cui, C.A. Tao, Y.G. Wu, Z.P. Li, L. Ma, Y.Q. Wen, G.T. Li, A strategy for producing pure single-layer graphene sheets based on a confined self-assembly approach, *Angew. Chem. Int. Ed.* 48 (2009) 5864–5868.
- [48] J. Lu, J.X. Yang, J. Wang, A. Lim, S. Wang, K.P. Loh, One-pot synthesis of fluorescent carbon nanoribbons, nanoparticles, and graphene by the exfoliation of graphite in ionic liquids, *ACS Nano* 3 (2009) 2367–2375.